Color transparency in the deuteron

V. V. Anisovich* and L. G. Dakhno
St. Petersburg Nuclear Physics Institute, 188350 Gatchina, Russia

M. M. Giannini†
Dipartimento di Fisica dell' Università, Genova, Italy
and Istituto Nazionale di Fisica Nucleare, Sezione di Genova, via Dodecaneso 33, I-16164 Genova, Italy
(Received 27 May 1993)

Quasielastic wide-angle *ep* scattering on the deuteron, the simplest reaction where color transparency can be investigated, is analyzed on the basis of multiple scattering theory. Color transparency reveals itself as a cancellation of elastic and inelastic shadowing. We calculate the energy dependence on the color transparency factor and the effects related to the Fermi motion. Extension of the results on other nuclei is also discussed.

PACS number(s): 13.60.−r, 12.38.Qk, 25.30.−c

I. INTRODUCTION

Color transparency means a disappearance of the initial and final state interactions of hadrons undertaking hard processes in nuclei, thus being a direct test of QCD [1,2]. This phenomenon gave rise to a lively discussion [3–5] which was mainly generated by the data of the BNL experiment [6] where wide-angle quasielastic *pp* scattering on nuclei (Li, C, Al, Cu, Pb) has been measured in the energy range $p = 6$–12 GeV/c. This experiment showed a puzzling behavior of the color transparency factor which increases in the momentum range 6–10, GeV/c and decreases at 12 GeV/c. Further investigations proved that (i) interference effects are important in the color transparency phenomenon, so it must be treated on a quantum mechanical level [7–10], and (ii) if the quasielastic *pp* scattering is considered on the quark level, not only single hard scattering [11,12] should be taken into account but the Landshoff multiple scattering as well [13] (see the discussion in Refs. [5,7,14]).

Wide-angle *pp* scattering data [6] were described quantitatively in Ref. [14] with the use of two mechanisms for the hard *pp* scattering: single hard scattering and Landshoff multiple one. Soft rescatterings were considered on the basis of the color screening phenomenon [15–17]: The gluon structure of the Pomeron [18] and its "small size" [19,20] allow one to formulate the concept of color screening in the language of Reggeon exchanges [21,22].

In order to interact weakly with nuclear matter the struck hadron configuration should have a size r_{cs} much smaller than the hadron one $R_{\rm hadron}$. The estimates of r_{cs} made in the analysis of soft hadron interactions [22] and in wide-angle quasielastic *pp* scattering [14] prove that $r_{cs}^2 \sim R_{\rm hadron}^2/10$. The corresponding momentum transfer squared is of the order of $Q^2 \sim 3$–5 GeV^2. Color transparency should appear in a single hard scattering just at such momentum transfers. However, there is one more parameter which governs the onset of color transparency, namely, the hadron energy before or after the hard interaction. Color transparency is switched on gradually with the increase of energy, in direct relation with the growth of inelastic rescatterings of the struck hadron. The problem of formation of hadron states involved in inelastic rescatterings is central for the occurrence of color transparency (for example, see the discussion in Refs. [23,24]). However, the mechanism of the transition from Glauber attenuation to color transparency was not yet clarified and for this end the language of hadron interactions and Reggeon exchanges, provided that color screening effects are taken into account, is expected to be helpful.

This paper is devoted to the study of color transparency with the use of a deuteron as the simplest example. In the process of deuteron electrodisintegration at large Q^2, $\gamma^* + d \to p + n$, all typical features of the color transparency phenomenon should reveal themselves in a rather simplified form. On the other hand, the technique of computation of hadron rescatterings is not too cumbersome. Therefore this example allows us to clarify some dark points: In particular, we shall analyze the role of inelastic shadowing and Fermi motion of nucleons in the formation of color transparency. To this end spin variables are not important and we neglect them. (The inclusion of spin variables needs a relativistic generalization of the deuteron wave function: see, for example, Ref. [25].)

In Sec. II the formulas for the deuteron disintegration amplitude are written, elastic and inelastic rescatterings being taken into account. Relying upon the idea of color transparency, we present the sum rule for this amplitude which provides a relation between shadowing and antishadowing contributions.

The inelastic shadowing amplitude depends on the effective mass M of the particles produced in the interme-

*Electronic address: anisovic@lnpi.spb.su
†Electronic address: giannini@genova.infn.it

diate state. At large M the M^2 dependence of this amplitude can be obtained in the framework of the dimensional counting rules [11,12]; however, the contribution of the low-energy masses is shrouded in uncertainty.

In Sec. III we try the models with a contrast M dependence in the low-mass region aiming to find a scale of changes in the preasymptotic behavior of the color transparency factor.

In Sec. IV a short summary of our results is given.

All the calculations have been performed using the language of hadron rescatterings (multiple scattering theory). Very important is to reformulate the problem, using the quark language; this subject is discussed in the Appendix.

II. SCREENING DIAGRAMS AND COLOR TRANSPARENCY

The investigation of color transparency in the deuteron electrodisintegration is being performed as follows. We consider first the case of quasielastic scattering of electrons on the target proton at rest (i.e., neglecting the Fermi motion), which corresponds to have the Bjorken variables $x_B = 1$. The color transparency is discussed in this kinematical situation and, as a consequence, we formulate a sum rule valid for high Q^2 and high energies of the outgoing proton. Then, using this sum rule, we calculate the energy dependence of the color transparency factor at all x_B.

Three diagrams determine the process of deuteron electrodisintegration (see Fig. 1). The impulse approximation diagram shown in Fig. 1(a) provides the main contribution to the amplitude, while the diagrams with final state interactions give comparatively small corrections. We assume the z axis parallel to the momentum p of the incoming electron. For high p and high momentum transferred along the z axis the proton is ejected practically at the same direction as the electron. The struck proton can rescatter softly off the spectator neutron and we approximate this amplitude by means of one Pomeron exchange [see Fig. 1(b)]. But another process is possible as well: The photon produces resonances (in general this leads to a shower of particles) which subsequently are transformed diffractively into the proton [see Fig. 1(c)]. As was pointed above, the diagrams shown in Figs. 1(b) and 1(c) are screening corrections with respect to the main contribution of the diagram of Fig. 1(a), but just these screening corrections are of great importance from the point of view of color transparency. They can be easily calculated in the framework of multiple scattering theory with inelastic rescattering taken into account (e.g., see Ref. [19]).

At large momentum transfer the photon selects a squeezed proton configuration which is colorless. Because of that its interaction with the spectator neutron vanishes in the limit of large momentum transfers and large energies of the struck proton. This means that in this limit the diagrams of Figs. 1(b) and 1(c) should cancel each other. The effect is similar to the one observed in hadron-deuteron scattering where Glauber and inelastic rescatterings give shadowing for low effective masses of the hadron shower [26,27], while the large-mass shower leads to antishadowing [28,29]. So it is reasonable to expect that the cancellation of diagrams of Figs. 1(b) and 1(c) is due to antishadowing contribution of not too small masses of the hadron shower in the process shown in Fig. 1(c).

Let the momenta of the incoming and outgoing electrons be $p_e = (p, 0, p)$ and $p'_e = (E', \mathbf{p}_\perp, p')$, where the electron mass has been neglected. In the laboratory frame which we use below $|\mathbf{p}_\perp|$ is large but $|\mathbf{p}_\perp| \ll p$, and p' is of the order of p. The Bjorken variables $x_B = Q^2/2m\nu$, where m is nucleon mass, is changing within the interval 0–2. In the impulse approximation one has the following condition for quasielastic ep scattering (the notations of momenta are shown in Fig. 1): $(q + P_d - k_2)^2 = m^2$, or $x_B \cong 1 + k_{2z}/m$. Here the nucleons of the deuteron are treated as nonrelativistic particles, and the lowest order terms are retained.

The deuteron blocks of the processes shown in Figs. 1(a)–1(c) neglecting terms of the order of k'^2_2 in the propagators of the struck proton and the produced resonances can be written respectively

$$A_{\mathrm{IA}} = 2\sqrt{m} F(Q^2) \Psi_d(\mathbf{k}_2^2), \tag{1}$$

$$A_{\mathrm{el}} = -i\sqrt{m} \int \frac{d^3k'_2}{(2\pi)^3} \Psi_d(\mathbf{k}'^2_2) F(Q^2) \frac{f((\mathbf{k}'_{2\perp} - \mathbf{k}_{2\perp})^2)}{k'_{2z} + i0}, \tag{2}$$

$$A_{\mathrm{in}} = -i\sqrt{m} \int \frac{d^3k'_2}{(2\pi)^3} \Psi_d(\mathbf{k}'^2_2) F_R(Q^2, M^2) \times \frac{f_{DD}((\mathbf{k}'_2 - \mathbf{k}_2)^2, M^2)}{k'_{2z} - (M^2 - m^2)/2(p - p') + i0} \tag{3}$$

Here A_{IA}, A_{el}, and A_{in} refer to the impulse approximation amplitude [Fig. 1(a)], elastic [Fig. 1(b)], and inelastic [Fig. 1(c)] rescattering amplitudes, correspondingly. $\Psi_d(\mathbf{k}'^2_2)$ is the deuteron wave function which depends on

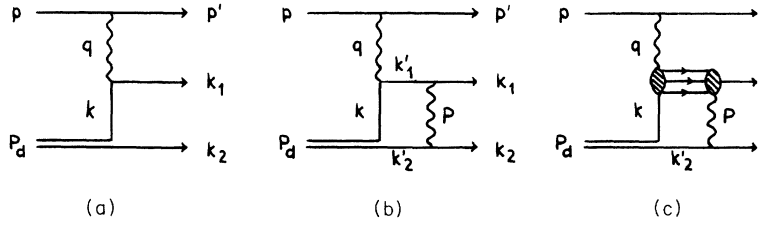

FIG. 1. Diagrams for the deuteron electrodisintegration process: (a) Impulse approximation diagram, (b) diagram with Glauber (elastic) rescattering, and (c) diagram with inelastic rescattering.

the square of the relative momentum of the nucleons and is normalized so that

$$\int \frac{d^3k}{(2\pi)^3}\Psi_d^2(k^2) = 1.$$

f is the amplitude for elastic pp scattering, while f_{DD} stands for the diffractive production of a resonance with mass M; F and F_R are the corresponding form factors. The elastic amplitude at small momentum transfers can be approximated as $f(k_\perp^2) \cong \sigma_{\rm tot}^{NN}\exp(-Bk_\perp^2/2)$, where $\sigma_{\rm tot}^{NN}$ is the total nucleon-nucleon cross section and B is the diffraction-cone slope. For the elastic rescattering of the nucleon, Eq. (2), we should make a substitution: $(k_z+i0)^{-1} \to -i\pi\delta(k_z)$, and for the diffraction resonance production one must substitute in Eq. (3)

$$[k_z - (M^2-m^2)/2(p-p') + i0]^{-1}$$

with

$$-i\pi\delta(k_z - (M^2-m^2)/2(p-p')).$$

Equation (3) stands for the amplitude of the diffractive production of a resonance with mass M on a bound nucleon. In the case of the production of several resonances one should sum up over all the resonances; for a continuous spectrum one has to integrate

$$\int_{M_0^2} \frac{dM^2}{\pi}\rho(M^2),$$

where M_0 is a threshold value and $\rho(M^2)$ is the density of the continuous spectrum. Such a procedure gives for the screening terms of Figs. 1(b) and 1(c) the following expression:

$$A_{\rm el}+A_{\rm in} = -\frac{1}{2}\sqrt{m}\int\frac{d^2k'_{2\perp}}{(2\pi)^2}\Psi_d(\mathbf{k}'^2_{2\perp})F(Q^2)f((\mathbf{k}'_{2\perp}-\mathbf{k}_{2\perp})^2) - \frac{1}{2}\sqrt{m}\int\frac{d^2k'_{2\perp}}{(2\pi)^2}\int_{M_2^2}\frac{dM^2}{\pi}\Psi_d\left(\mathbf{k}'^2_{2\perp}+\frac{(M^2-m^2)^2}{4(p-p')^2}\right)$$
$$\times F_R(Q^2,M^2)\rho(M^2)f_{DD}((\mathbf{k}'_{2\perp}-\mathbf{k}_{2\perp})^2 + (M^2-m^2)^2/4(p-p')^2, M^2). \quad (4)$$

In the above equation the contribution of resonances is not shown separately but is included in the density $\rho(M^2)$. The values of M^2 can be rather large, $M^2 \sim (p-p')\sqrt{m\varepsilon}$, since the deuteron wave function allows for $|k_z|$ the value of the order of $\sqrt{m\varepsilon}$ (ε is the deuteron binding energy).

The integrand in the inelastic shadowing term given by Eq. (4) can be presented as a discontinuity of the amplitude $A_{\gamma N}$ in the M^2 channel: $i2m(p-p')F_R\rho f_{DD}=\mathrm{disc}_{M^2}A_{\gamma N}$. It is hardly possible to derive the M^2 dependence of $\mathrm{disc}_{M^2}A_{\gamma N}$ in the region of low and intermediate M; however, it is possible to find out asymptotic behavior of $\mathrm{disc}_{M^2}A_{\gamma N}$ at large M^2 and Q^2 using the language of quarks (see Appendix).

To simplify the following presentation let us neglect in Eq. (4) the momentum transfer dependence in the diffractive interactions, $\kappa^2 = (\mathbf{k}'_2-\mathbf{k}_2)^2 \to 0$. It is a good approximation if the range of the final state interaction of nucleons is much smaller than the deuteron size. (Actually there is no special need in this simplification and in our calculation of the transparency factor we restore the momentum transfer dependence.) Then the rule for the asymptotic cancellation of the screening terms of the amplitude, in the limit of large $p-p'$ and Q^2, reads as

$$0 = F(Q^2)\int\frac{d^2k_\perp}{(2\pi)^2}\Psi_d(k_\perp^2)f(0,s_N) + \int_{M_0^2}^{M^2_{\max}}\frac{dM^2}{\pi}\int\frac{d^2k_\perp}{(2\pi)^2}\Psi_d\left(k_\perp^2+\frac{(M^2-m^2)^2}{4(p-p')^2}\right)\frac{\mathrm{disc}_{M^2}A_{\gamma N}(Q^2,M^2,s_N)}{is_N}, \quad (5)$$

where $s_N = 2m(p-p')$. Equation (5) must be valid for all large values of Q^2 and this means that the ratio $A_{\gamma N}/F(Q^2)$ is independent of Q^2. Actually such a cancellation is a direct consequence of the dimensional counting rules [11,12] and it is valid for all M. The energy dependence of the elastic scattering amplitude $is_N f(0,s_N)$, and for the amplitude $A_{\gamma N}(M^2,Q^2,s_N)$, must be the same as well: Pomeron exchange in both amplitudes guarantees it.

III. ENERGY DEPENDENCE OF THE COLOR TRANSPARENCY FACTOR

Our knowledge of the Glauber screening and large-M behavior of the final state interaction block allows us to construct models which make it possible to find out the scale of changes in the preasymptotic behavior of the color transparency factor. Two factors determine the asymptotics of $\mathrm{disc}_{M^2}A_{\gamma N}$: the M dependence of the amplitude γ+nucleon→nucleon+Pomeron which behaves as M^{-4} (see Appendix) and Pomeron exchange amplitude for inelastic rescattering, is_N/M^2. Thus, at large M $\mathrm{disc}_{M^2}A_{\gamma N} \sim M^{-6}$. We approximate $\mathrm{disc}_{M^2}A_{\gamma P}$ as

$$\mathrm{disc}_{M^2}A_{\gamma N}(M^2,Q^2,s_N) = F(Q^2)is_N\varphi(M^2), \quad (6)$$

where

$$\varphi(M^2) = \theta(M-M_0)\theta(M_1-M)\Phi(M^2) + \theta(M-M_1)\Phi(M_1^2)(M_1/M)^6. \quad (7)$$

Here $\Phi(M^2)$ is a function which describes the M dependence in the resonance region ($M_0 < M < M_1$), while the asymptotic decrease, M^{-6}, starts at $M = M_1$. To make

clear the influence of this resonance region on the transparency onset as well as to estimate uncertainties which come from it, we consider two extreme cases: (I) Resonance domain is large, $M_0^2 \simeq 2$–3 GeV^2, $M_1^2 \simeq 10$–12 GeV^2, and its contribution is not small. (II) Asymptotic decrease of $\mathrm{disc}_{M^2} A_{\gamma N}$ starts at small M^2, thus $M_1^2 \simeq M_0^2 = 2$–3 GeV^2.

In our calculation $f(0, s_N) = \sigma_{\mathrm{tot}}^{NN} = 39$ mb and $M_{\max}^2 = m_N \sqrt{s_N}$. The results for inelastic shadowing at large ν do not depend practically on the value of $M_{\max}^2$ because the main contribution comes from not too high M^2.

Up to now we considered the case $x_B = 1$ which corresponds in the quasielastic kinematics to the target nucleon with $k_z = 0$. It is easy to rewrite the amplitude for $x_B \neq 1$:

$$(2\sqrt{m}F(Q^2))^{-1} A = \Psi_d(k_\perp^2 + m^2(1-x_B)^2) - \frac{\sigma_{\mathrm{tot}}^{NN}}{16\pi} \int_0^\infty dk_\perp'^2 \Psi_d(k_\perp'^2 + m^2(1-x_B)^2)$$
$$- \frac{1}{16\pi} \int_0^\infty dk_\perp'^2 \int_{M_0^2}^{M_{\max}^2} \frac{dM^2}{\pi} \Psi_d\left(k_\perp'^2 + m^2\left(x_B - 1 + \frac{M^2 - m^2}{s_N}\right)^2\right) \varphi(M^2). \quad (8)$$

The case with $k_z = m(x_B - 1) < 0$ corresponds to the target nucleon moving in the direction opposite to the incoming electron.

For reaction with deuteron as a target we should better consider for the color transparency factor a slightly different definition as compared to the usual one for intermediate and heavy nuclei. We write

$$T_d = \frac{\int d^2k_\perp \sigma_d(x_B, \nu, Q^2, k_\perp^2)}{\int d^2k_\perp \sigma_{\mathrm{IA}}(x_B, \nu, Q^2, k_\perp^2)}, \quad (9)$$

where σ_d is the cross section $ed \to epn$ [i.e., with the amplitude defined by Eq. (8)] and σ_{IA} is the cross section in the impulse approximation only. T_d depends on x_B and ν, the Q^2 dependence being canceled at $Q^2 > 3$–5 GeV^2 (corrections of the order of $\ln Q^2$ have been neglected here). The values of T_d for different x_B and ν are shown in Fig. 2. The results have been obtained using the Reid soft core wave function (we define Ψ_d as either $\sqrt{\Psi_S^2 + \Psi_D^2}$ or Ψ_S) and remain practically unchanged if the Paris potential is used.

Calculated values of T_d for cases I and II are shown in Figs. 2(a) and 2(b). We denote the transparency factor for this model as $T_d(M_0^2, M_1^2)$ [see Eq. (7)]. In case I, when the resonance region with antishadow contribution is rather broad ($M_0^2 = 2$ GeV^2, $M_1^2 = 12$ GeV^2), T_d increases rather slowly with energy: at $\nu = 10$ GeV the screening terms cancel each other in 20–25% only, while for a 50% cancellation the energy transfer must be of the order of 20–70 GeV. Fermi motion, which reveals itself at $x_B \neq 1$, changes the rate of increase of T_d a little: at $x_B = 0.9$ the increase in the region of $\nu \simeq 5$–10 GeV is slightly quicker than at others x_B, but for $\nu > 15$ GeV the rate of increase is almost the same for all x_B. The values of T_d with $|x_B - 1| \sim 0.3$–0.5 behave similarly, being weakly dependent on the sign of $x_B - 1$, see Fig. 2(b). In case II, when the resonance region is narrow ($M_0^2 = M_1^2 = 3$ GeV^2), the transparency factor T_d is sensitive to the Fermi motion: the 50% decrease of shadowing occurs for $x_B \leq 0.9$ at $\nu = 8$–10 GeV while for $x_B \geq 1$ it happens at $\nu = 20$–30 GeV only.

Up to now we were dealing with rather specific case (while being the most favorable for the onset of the color transparency): all the inelastic production gave antishadowing contributions. We have also studied the case where the production of a resonance was of a shadow type and then the contribution of higher masses was antishadowing. For this case the calculation results are presented in Figs. 2(c) and 2(d) for the shadowing resonance with mass $M_{\mathrm{res}}^2 = 2$ GeV^2 and with reasonable cross-section value (about 1/3–1/2 of the elastic one). Color trans-

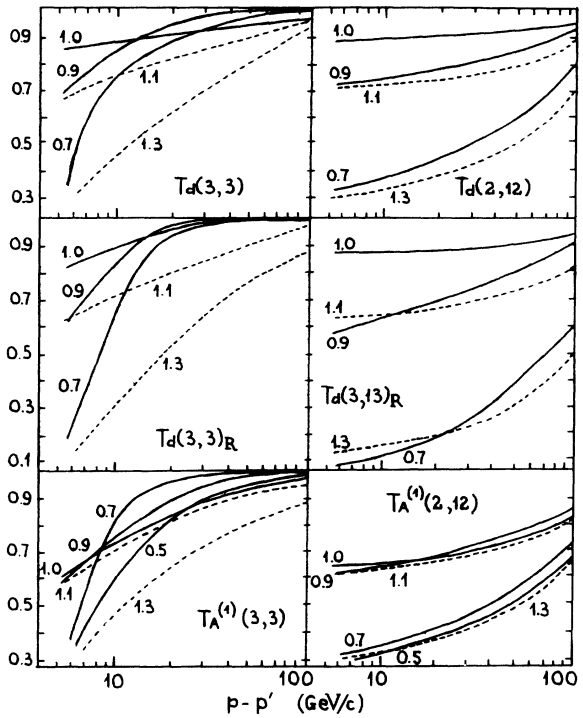

FIG. 2. (a),(b) Transparency factor given by Eq. (9), $T_d(M_0^2, M_1^2)$, as a function of ν for Reid soft core wave function. M_0^2 and M_1^2 define the region of the nonasymptotic behavior of $\varphi(M^2)$ which enters Eq. (7); $\Phi(M^2)$ =const. Solid curves correspond to x_B=0.5, 0.7, 0.9, and 1; dashed curves stand for $x_B = 1.1$ and 1.3 (c),(d). The same as in (a),(b) but with additional shadowing resonance contribution ($M_{\mathrm{res}}^2 = 2$ GeV^2). (e),(f) The same as in (a),(b) but for the nuclear transparency factor, $T_A^{(1)}(M_0^2, M_1^2)$, defined by the diagrams of Figs. 3(a), 3(b), 3(c). Two-nucleon correlation factor is taken from Ref. [30].

parency factor for this model is denoted as $T_d(M_0^2, M_1^2)_R$. One can see that the shadowing contribution of resonances does not change the whole picture—the approach to the transparency limit is very similar to that considered previously.

Our results can be extended to a nucleus target with $A > 10$. In the approximation where the nucleus is considered as a dilute system of nucleons (it is standard approximation of the Glauber theory) the amplitude on a nucleus is given by a set of diagrams of Fig. 3 type: the diagrams of Figs. 3(a)–3(c) are the same as in the case of the deuteron target while Fig. 3(d) describes the subsequent rescatterings of the struck proton or the proton-induced shower. It seems reasonable to assume that the rate of growth of the transparency factor T_A is qualitatively the same both in the diagrams of Figs. 3(b) and 3(c) (one-rescattering process) and in diagrams with multiscatterings [Fig. 3(d) type]. The influence of Fermi motion can be also checked in the example of the one-rescattering diagrams of Figs. 3(b) and 3(c). In Figs. 2(e) and 2(f) one can see the results of the calculation of the nuclear transparency factor with one rescattering, $T_A^{(1)}$: in this case the value $T_A^{(1)}$ is defined by the same formulas but with ψ_d substituted by the two-nucleon correlation wave function [30]. One can see that at small ν the screening corrections are larger than in the deuteron case (because of larger nuclear density). However, the decrease of shadowing for increasing ν and the x_B dependence of $T_A^{(1)}$ are practically the same as in the deuteron case.

The factor $T_A^{(1)}$ integrated over k_z near $x_B = 1$ does not demonstrate a change of the energy-dependent behavior as compared to the case of $x_B = 1$: $\langle T_A \rangle = \int dk_z T_A^{(1)}$ increases in the region $\nu = 5$–15. Such a behavior of $\langle T_A \rangle$ is an argument against the explanation of the BNL puzzle as a result of the Fermi motion [24]. Let us discuss this point in more detail. In Ref. [6] two kinds of transparency factors are presented: (i) after reconstruction of Fermi motion of the target nucleon (neglecting binding energy and initial or final state interactions), (ii) without it but integrating in the range -0.2 GeV/$c < k_z < 0.1$ GeV/c. Although the first kind of representation might be criticized [24], the second one looks appropriate. The color transparency factor, which has been found in accordance with the prescription (ii), increases in the region of $p = 6$–10 GeV/c and decreases at $p = 12$ GeV/c. It looks reasonable to assume that Fermi motion reveals itself similarly in both wide-angle quasielastic ep and pp reactions. If so, our calculation which shows monotonic growth of $T_A^{(1)}$, indicates that BNL puzzle is of another origin, not a simple influence of the Fermi motion. Another possibility to explain BNL puzzle has been discussed in Refs. [5,7,14] where it was related to a significant contribution of the Landshoff multiple scattering to the wide-angle elastic pp amplitude at intermediate energies. This emphasizes the necessity to investigate electromagnetic hard processes such as the quasielastic ep scattering on nuclei where the Landshoff mechanism is absent; on the other hand, further information should be obtained from the analysis of reactions with multinucleon emission, say $(e, e'NN)$, at high Q^2 where the pp interaction could be once more important.

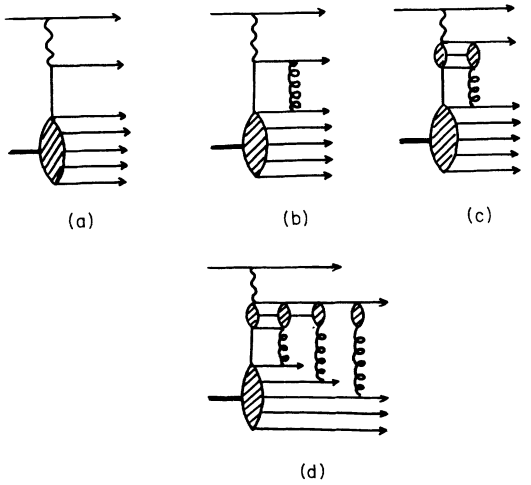

FIG. 3. Diagrams for quasielastic eA scattering: (a) Impulse approximation diagram, (b), and (c) diagrams corresponding to the one-rescattering process, and (d) diagrams with multirescatterings.

IV. CONCLUSION

Color transparency has been considered in the deuteron electrodisintegration where all screening corrections have been calculated using standard multiple scattering techniques. The approach was substantially based on hadron concepts and dynamics, while a reference to quarks is implicitly contained in the requirement that screening correction should vanish at very high energy momentum transfers. Starting from this color transparency limit, when shadow (or Glauber) corrections are canceled by antishadow terms related to the inelastic scattering of a struck nucleon, we calculated the behavior of the screening corrections as a function of the energy transferred to the deuteron, ν. The calculations prove that the rate of the color transparency growth with ν depends on the contribution of resonances in the inelastic antishadow rescattering. Dominant contribution of the low-mass resonances increases this rate as well as its sensitivity to the Fermi motion: at $x_B < 1$ the transparency factor grows faster than at $x_B > 1$. Quite opposite is the case, when antishadow contributions are related to highly excited resonances with $M \sim 2$–3 GeV, the rate of the color transparency growth is dumped, and the influence of the Fermi motion is suppressed as well. But in all the cases the onset of color transparency is very slow—one-half of the Glauber screening correction is canceled not earlier than at $\nu = 10$–20 GeV. Thus, the investigation of color transparency by means of quasielastic electron-nucleon processes—just this reaction is the best for interpretation—is a task not only for the intermediate-energy accelerators but also for the next generation ones as well as for DESY.

ACKNOWLEDGMENTS

Thanks are due to D. I. Melikhov and M. G. Ryskin for fruitful discussions. Two of us (V.V.A and L.G.D.) are grateful for the hospitality at the National Institute of Nuclear Physics (INFN) (Sezione di Genova) and at the Physics Department of the University of Genova. This work was supported by the Russian Research Grant No. 93-03-3852.

APPENDIX A: QUARK MODEL FOR INTERACTION AMPLITUDE

Here the interaction amplitude $\gamma + N \to N + P$ (P is a Pomeron), which contains principal features of the color transparency phenomenon, is investigated by means of a quark language.

Let us denote the amplitude of the interaction block, which is a sum of diagrams of Figs. 4(a) and 4(b), as $a(\gamma N \to NP)$. The amplitude $A_{\gamma N}$ in Eq. (5) is a product of this amplitude and the Pomeron propagator: $A_{\gamma N} = i(s/M^2)a(\gamma N \to NP)$. Therefore, for the calculation of the cross section we need to know $\mathrm{disc}_{M^2} a(\gamma N \to NP)$. In the proposed model the amplitude $a(\gamma N \to NP)$ is represented as a quark diagram shown in Fig. 4(c). H is the hard interaction block which is a sum of diagrams of the type of Fig. 4(d) (the detailed consideration of hard exclusive processes may be found in Ref. [31]): exchanges of hard gluons g give the momenta of outgoing quarks about $q/3$. The block S, which describes soft quark Pomeron scattering, is a sum of diagrams of Figs. 4(e) and 4(f) type in the leading $1/N_c$ approximation. The diagram with Pomeron exchange gives shadowing while three-regeon diagram of Fig. 4(f), GGP, where G Reggeized gluon, gives antishadowing. The whole soft scattering amplitude, $S = \sum(P + GGP)$, vanishes, when the transverse interquark distances tend to zero [32]. After cutting the diagram of Fig. 4(c) between hard and soft blocks (dashed line), we get the discontinuity of the amplitude in the M^2 channel which enters shadowing corrections, Eq. (5).

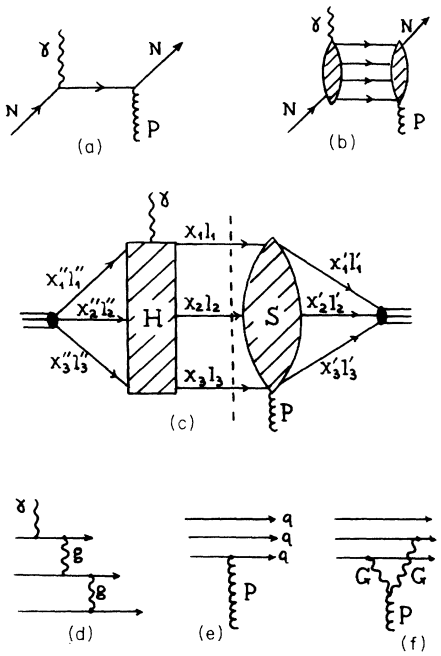

FIG. 4. (a),(b) Elastic and inelastic rescattering blocks, presented in the hadron language. (c) Representation of the sum of (a) and (b) as a quark interaction diagram: H is a hard scattering block and S is a soft scattering one [see Eq. (A1)]. (d) An example of quark diagram which defines hard scattering block H: the exchange of hard gluons distributes the photon momentum among three quarks. (e),(f) Diagrams for soft scattering of outgoing quarks (block S): shadowing (e) and antishadowing (f) diagrams.

At large Q^2 the diagram shown in Fig. 4(c) is similar to that of the proton form factor. The only difference from the form factor is that outgoing quarks interact with another nucleon by the Pomeron exchange. Similar to the form factor process the amplitude of the hard exclusive reaction $\gamma N \to NP$ is obeying the factorization formula which separates the hard scattering amplitude H from the bound state dynamics and the soft rescattering process. Correspondingly, the discontinuity of the amplitude in the M^2 channel can be written as

$$\mathrm{disc}_{M^2}(\gamma N \to NP) = \int d\Phi(x'', r_\perp'')\psi_N(s'')H(x'', x; Q)d\Phi(x, r_\perp)\delta\left(M^2 - \sum \frac{m_{i\perp}^2}{x_i}\right) S(x, r_\perp; x', r_\perp')\psi_N(s')d\Phi(x', r_\perp'), \tag{A1}$$

where $(x'', r_\perp'')$ and $(x', r_\perp')$ are the light-cone variables of the incoming and outgoing quarks, respectively: $x'' = k_+''/k_+$, $x' = k_+'/k_{1+}$, and $d\Phi$ is the three-quark phase space,

$$d\Phi = \prod_{i=1}^{3}\left(\frac{dx_i}{x_i} d^2 r_{i\perp}\right)\delta\left(1 - \sum x_i\right)\delta^2\left(\sum r_{i\perp}\right).$$

The nucleon wave function depends on the energy squared of three quarks. The hard block H decreases as Q^{-4} in the leading order in $1/Q$ selecting small relative distances between quarks, $|\mathbf{r}_{i\perp}| \sim 1/Q$. Soft scattering block S contains two types of terms which are shown in Figs. 4(e) and 4(f). In the $r_\perp$ representation this interaction leads to the factor $(3 - \sum_{i \neq j} \exp[-(\mathbf{r}_{i\perp} - \mathbf{r}_{r\perp})^2/4r_{cs}^2])$, where the quantity 3 comes from diagrams of Fig. 4(e) and the second term is the contribution of three Reggeon diagram. The parameter r_{cs}^2 is of the order of 0.6 GeV^{-2} [14]. Hard interaction and soft scattering cancel the final state interaction block of Fig. 4(c) at $r_{cs}^2 Q^2 \gg 1$.

At small Pomeron momentum, κ, the M^2 dependence

of Eq. (A1) for large M^2 is $\mathrm{disc}_{M^2} a(\gamma N \to NP)/Q^4 \sim M^{-4}$. Actually the asymptotic M^2 behavior of the amplitude shown in Fig. 4(c) depends on the number of quarks, and in this sense it is similar to the form factor behavior: for example, for mesons $\mathrm{disc}_{M^2} a(\gamma + \text{meson} \to P + \text{meson})/Q^2 \sim M^{-2}$. Actually this follows from dimensional counting rules [11,12] as well.

Thus, this model gives the expected by QCD cancellation of screening effects at large Q^2 and p_N. Now let us explain how this model is linked with the multiple scattering theory used in our calculations.

Unitarity condition for the amplitude $a(\gamma N \to NP)$ reads

$$\mathrm{disc}_{M^2} a(\gamma N \to NP) = \sum_{\text{hadrons}} A^*(\gamma N \to \text{hadrons}) \times A(\text{hadrons} \to NP). \quad \text{(A2)}$$

In the unitarity condition the summation is initially going over all hadron states, but the constraints imposed to amplitudes $A^*(\gamma N \to \text{hadrons})$ and $A(\text{hadrons} \to NP)$ by the conservation laws allows us to restrict the summation to a limited set of states. For example, the process $\gamma N \to$ hadrons allows for hadrons the isotopic states $I = 1/2$ and $I = 3/2$; however, the amplitude $A(\text{hadrons} \to NP)$ with $I = 3/2$ is equal to zero, hence the states $I = 3/2$ go away from the final summation.

Consider a model when only three-quark baryon states are taken into account in the intermediate state of Eq. (A2) (for example, those which are discussed in the quark model calculations, see [33,34] and references therein). So we redraw the sum of diagrams shown in Figs. 4(a) and 4(b) as a diagram of Fig. 5(a), summing over all baryon resonances, nucleon state included as well. The wave functions of the three-quark baryons can be presented as a full set of states in the three-quark state space:

$$\sum_n \psi_n(\mathbf{r}_{\perp 1}, x_1; \mathbf{r}_{\perp 2}, x_2; \mathbf{r}_{\perp 3}, x_3) \times \psi_n^*(\mathbf{r}_{\perp 1}, x_1; \mathbf{r}_{\perp 2}, x_2; \mathbf{r}_{\perp 3}, x_3) = \hat{I}, \quad \text{(A3)}$$

where $\hat{I}$ is a unity operator. This is how the sum of diagrams of Fig. 5(a) comes into the diagram of Fig. 4(c).

Two remarks have to be made.

(i) We explore the completeness condition for the baryon wave functions just as it could be used in nuclear physics for three-nucleon states. Generally speaking, there is an essential difference related to the constraint due to confinement of quarks. However, we discuss here small interquark distances, so—one may believe—we may forget about the confinement constraints.

(ii) The constraint in the summation of the set of states exists not only in Eq. (A2) but in the quark diagram of Fig. 4(c) as well. For example, intermediate states with $I = 3/2$ are absent in the diagram of Fig. 4(c): conservation law in soft scattering amplitude guarantees it.

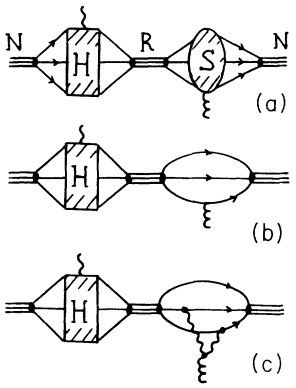

FIG. 5. (a) Final state interaction block, $a(\gamma N \to NP)$, written as a sum over three-quark resonances, R, in the intermediate state. Diagrams which give the shadow contribution (b) and antishadow one (c).

Consider in more detail the diagram of Fig. 5(a). Soft scattering block S includes two types of interactions, so the diagram of Fig. 5(a) is a sum of diagrams of Figs. 5(b) (shadowing) and 5(c) (antishadowing). Now it is seen that color transparency effect in the final state interaction amplitude appears as a cancellation of contributions of low-mass nucleon states and highly excited ones. Indeed, in the case of negligibly small momentum transferred by Pomeron, κ, the only nucleon state ($R = N$) gives nonzero contribution in the set of diagrams 5(b): the soft scattering block RPN is equal to zero for $R \neq N$ because of the quark wave function orthogonality. The diagram of Fig. 5(b) with $R = N$ gives shadowing contribution: it is usual Glauber screening diagram. The diagrams of Fig. 5(c) provides the contribution of the opposite sign. However, the diagram on Fig. 5(c) with $R = N$ is a comparatively small correction to the contribution of the diagram of Fig. 5(b) with $R = N$ and does not change the shadowing nature of the Glauber scattering. But the other terms of the diagram of Fig. 5(c) with $R \neq N$ are also nonzero: they are negative and the sum of all these terms exactly cancels the Glauber screening at large Q. It is also seen that this cancellation happens only at a large enough ν, when the deuteron wave function does not cut the contribution of nonsmall masses.

In principle it is possible to calculate the final state interaction block of Fig. 5 if the wave functions of nucleon states R are known. In the last decade considerable progress has been made in the baryon spectroscopy as well as in the consideration of form factors (see, correspondingly, Refs. [33,34] and Refs. [35,35]). However, it is a long-term problem.

[1] A. H. Mueller, in *Proceedings of XVII Rencontre de Moriond*, Moriond, 1982, edited by J. Tran Than Van (Editions Frontiers, Gif-sur-Yvette, France, 1982), p. 13.

[2] S. J. Brodsky, in *Proceedings of XIII Symposium on Multiparticle Dynamics*, edited by W. Kittel, W. Metzger, and A. Stergion (World Scientific, Singapore, 1982).

[3] G. R. Farrar, H. Liu, L. L. Frankfurt, and M. I. Strikman, Phys. Rev. Lett. **61**, 686 (1988).

[4] S. J. Brodsky and G. F. deTeramond, Phys. Rev. Lett. **60**, 1924 (1988).

[5] J. P. Ralston and B. Pire, Phys. Rev. Lett. **61**, 1823 (1988).
[6] A. S. Carrol *et al.*, Phys. Rev. Lett. **61**, 1698 (1988).
[7] J. Botts, Phys. Rev. D **44**, 2768 (1991).
[8] J. P. Ralston and B. Pire, Phys. Rev. Lett. **65**, 2343 (1990).
[9] B. K. Jennings and G. A. Miller, Phys. Rev. D **44**, 692 (1991).
[10] J. P. Blaizot, R. Venugopalam, and M. Prakash, Phys. Rev. D **45**, 814 (1992).
[11] V. A. Matveev *et al.*, Lett. Nuovo Cim. **7**, 719 (1973).
[12] S. J. Brodsky and G. R. Farrar, Phys. Rev. Lett. **31**, 1153 (1973).
[13] P. V. Landshoff, Phys. Rev. D **10**, 1024 (1974).
[14] V. V. Anisovich, L. G. Dakhno, V. A. Nikonov, and M. G. Ryskin, Phys. Lett. B **292**, 169 (1992).
[15] S. Nussinov, Phys. Rev. Lett. **34**, 1286 (1975).
[16] F. E. Low, Phys. Rev. D **12**, 163 (1975).
[17] J. F. Gunion and D. E. Soper, Phys. Rev. D **15**, 2617 (1977).
[18] L. N. Lipatov, Zh. Eksp. Teor. Fiz. **90**, 1536 (1986) [Sov. Phys. JETP **63**, 904 (1986)].
[19] V. V. Anisovich, M. N. Kobrinsky, Y. Nyiri, and Yu. Shabelski, *Quark Model and High Energy Collisions* (World Scientific, Singapore, 1985).
[20] P. V. Landshoff and O. Nachtman, Z. Phys. C **35**, 405 (1987).
[21] V. V. Anisovich and M. M. Giannini, Z. Phys. C **50**, 441 (1991).
[22] V. V. Anisovich, L. G. Dakhno, and V. A. Nikonov, Phys. Rev. D **44**, 1385 (1991).
[23] A. Bianconi, S. Boffi, and D. Kharzeev, Report No. FNT/T-92/38, Pavia, 1992.
[24] B. K. Jennings and B. Z. Kopeliovich, Report No. PP-92-95, Vancouver, 1992.
[25] V. V. Anisovich, M. N. Kobrinsky, D. I. Melikhov, and A. V. Sarantsev, Nucl. Phys. **A544**, 747 (1992).
[26] J. Pumplin and M. Ross, Phys. Rev. Lett. **21**, 1778 (1968).
[27] V. N. Gribov, Zh. Eksp. Teor. Fiz. **56**, 892 (1969) [Sov. Phys. JETP **29**, 483 (1969)].
[28] V. V. Anisovich, L. G. Dakhno, and P. E. Volkovitsky, Phys. Lett. B **42**, 224 (1972).
[29] A. B. Kaidalov and L. A. Kondratyuk, Nucl. Phys. **B56**, 90 (1973).
[30] C. Ciofi degli Atti, S. Liuti, and S. Simula, Phys. Rev. C **41**, R2474 (1990) and private communication.
[31] G. P. Lepage and S. J. Brodsky, Phys. Rev. D **22**, 2157 (1980).
[32] V. V. Anisovich and L. G. Dakhno, Nucl. Phys. (Proc. Suppl.) **B25**, 247 (1992).
[33] S. Capstick and N. Isgur, Phys. Rev. D **34**, 2809 (1986).
[34] S. K. Sharma, W. H. Blask, B. C. Metsch, and M. G. Huber, Phys. Rev. Lett. **62**, 2913 (1989).
[35] R. Eckardt, J. Hansper, and M. F. Gari, Z. Phys. A **343**, 443 (1992).
[36] M. Bergmann and N. Stefanis, Phys. Rev. D **47**, R3685 (1993).